A computational exploration of the color gamut of nanoscale hollow scalene ellipsoids of Ag and Au

*Catherine S. Kealley, Michael B. Cortie**

Institute for Nanoscale Technology, University of Technology Sydney, PO Box 123, Broadway, NSW 2007, Australia

michael.cortie@uts.edu.au

Running head: color gamut of hollow scalene ellipsoids of Ag and Au

RECEIVED DATE (automatically inserted by publisher);

ABSTRACT

Hollow, nanoscale, scalene ellipsoids of Ag or Au provide an exceedingly tunable localized surface plasmon resonance. Here we use numerical simulations to determine the limits of the color space that would be possible from colloidal suspensions of these particles, and show that their color gamut will exceed that possible with nanorods, nanoshells or nanorice. The important parameters are composition, thickness of the shell and shape of the particle, in that order. The sensitivity of colors to geometry is optimized for an aspect ratio of between 0.3 to 0.5 and was reduced for thinner shells. Shells of Ag will have much wider and more vibrant gamut than those of Au. These findings indicate that hollow scalene ellipsoids could be used as versatile pigments in materials or display systems that exploit plasmon resonance to produce color.

KEYWORDS gold and silver nanoshells, scalene ellipsoid, plasmon resonance, color gamut

Introduction

Metallic nanostructures have attracted considerable attention because of their plasmonic, catalytic or electronic properties. In particular, nanoparticles of Au and Ag have unique and interesting optical properties in the visible and near-infrared regions of the spectrum (Kelly et al., 2003). The plasmonic properties stem from the interaction of light with the free electrons in the metal nanoparticle giving rise to localized surface plasmons, which lead to the selective absorption and scattering of particular wavelengths of light. Hence, if the phenomena occur in the visible part of the spectrum, there is a resulting color visible to the naked eye. Diverse applications, such as chemical and biomolecular sensing, nanoscale optical components or devices, and surface-enhanced spectroscopies exploit this phenomenon (Wang et al., 2006). The plasmon resonance frequencies of a metallic nanoparticle are dependent on the particle's composition, size, shape, and surface topography (Kelly et al., 2003).

It has been reported (Wang et al., 2006) that a 'nanorice' particle would combine the intense local fields from nanorods with the highly tunable plasmon resonances of nanoshells. To tune the plasmon resonance frequency of nanorods, the length or aspect ratio of the nanorod is varied (Yu et al., 1997). For nanoshells, the relative size of the inner and outer radius of the metallic shell layer is adjusted (Oldenburg et al., 1998, Prodan and Nordlander, 2004). In the reported 'nanorice' particle, $a=b\neq c$, where a and b are the equatorial radii and c the polar radius. For 'nanorice' consisting of a spheroidal Au or Ag shell which encloses a spindle-shaped dielectric core, it was found that the plasmon tunability arising from varying the thickness of the shell layer was far more greater than that arising from varying the length of the nanostructure (*ie.* ratio of a to c) (Wang et al., 2006).

It is possible to envisage an even more flexible particle than a 'nanorice', specifically, a hollow scalene ellipsoid in which $a\neq b\neq c$, obtained by relaxing the geometry of the nanorice by one further degree of freedom. In the present work we have sought to determine just how widely the optical response of such an ellipsoidal nanoparticle can be tuned. The exercise has been carried out by computer simulation of aqueous colloids of the hypothetical particles.

Methodology

1. Simulation of Concentric Ellipsoids

We have simulated the optical properties of the proposed nanoscale, hollow, scalene ellipsoids using DDSCAT, the code of Draine and Flatau that exploits the discrete dipole approximation (Draine and Flatau, 1994, Draine and Flatau, 2004). In this scheme the optical behavior is obtained numerically. The applicability and accuracy of this technique has been previously verified by various investigators (Brioude et al., 2005, Felidj et al., 1999, Kelly et al., 2003), and its particular advantage is that it can be applied to arbitrarily-shaped particles. A linear response of the material to an electric field is assumed in the code used. Furthermore, here we have used the bulk dielectric constant, and neglected surface scattering. We will comment on the significance of this latter approximation later. The particle is approximated by an array of polarisable points, so it is important to use a fine mesh in order to obtain a reasonable rendition of fine detail. However, in practice, the array size (and hence accuracy) is limited by available computational resources and time. At each point of the grid there is a dipole with polarisability corresponding to the chosen material. The response of this array of dipoles to an incident field is then determined self-consistently from which the extinction can be calculated.

Calculations were performed using the published complex refraction indices of gold, silver and water (Weaver and Frederikse, 2001). A one nanometer dipole spacing (about 33,000 dipoles per particle) was applied in the calculations. A typical target rendered at this resolution is shown in Figure 1(a). This is generally considered to be sufficiently fine for most shapes (He and Shi, 2005) but, to check this, we repeated sample calculations at finer dipole spacings down to 0.5 nm, Figure 1(b). It is apparent that the extinction peaks sharpen somewhat if re-calculated at a higher resolution. However, given that the monodispersity assumed here for the colloidal particles is unattainable in practice anyway, any actual extinction peaks that would be obtained in a real suspension would be less intense and broader than even those calculated for the 1 nm dipole spacing. Therefore, we considered use of the

1 nm dipole spacing to be justified. The calculations were repeated for light polarized along each of the axes of the target, and the results combined with a weighted average. The calculated optical properties are expressed in terms of extinction efficiency, Q_{ext}. In the case of the DDSCAT code, this is the ostensible optical extinction cross-section normalized by the nominal geometric cross-sectional area of the particle, expressed as if all the matter in the particle was packed into a sphere (Draine and Flatau, 2004). Colors in the Commission Internationale de I'E Clairage (CIE) color model were directly calculated from spectra using appropriate tables (American Society for Testing and Materials, 2001), after converting the calculated Q_{ext} to a percentage transmission based on the density of nanoparticles present in a colloidal suspension using:

$$A = \frac{N.C_{ext.}x}{2.303} \qquad (1)$$

where A is the solution absorbance, N the number of particles per unit volume, C_{ext} the extinction cross-section, and x the optical path length (Perez-Juste et al., 2005). Colors were assessed at a concentration corresponding to $3x10^{16}$ nanoparticles per m^3. In the CIE LAB system the L coordinate refers to the luminance of the color, the a^* measures the green-to-red tendency of the color, and the b^* the blue-to-yellow tendency. The white point is given by $a^* = b^* = 0$. The L-a^*-b^* colors were then converted through CIE XYZ to RGB using the matrices given by Pascale (Pascale, 2003). Note that the calculated colors err slightly on the side of being more intense than would be expected from real world particles. This is because actual ellipsoidal particles would not be perfectly monodisperse and because, in the case of very thin-walled targets, surface scattering of the plasmon would tend to reduce color saturation. Color charts were drawn by sampling the parameter space at 10 nm intervals (or more closely if the color varied rapidly with dimension).

2. Selection of Metals

A wide range of elements and compounds have dielectric properties that will provide a plasmon resonance (Blaber et al., 2007). Sodium and potassium nanoshells, in particular, have dielectric properties that would provide a strong localized plasmon resonance in the visible part of the spectrum (Blaber et al., 2009). Unfortunately, the extreme chemical reactivity of these elements precludes their use is atmospheric or aqueous environments, while nanoparticles of other, more noble elements such as copper or platinum, have indifferent or absent plasmon resonances (Cortie et al., 2006). Compounds such as $AuAl_2$ (Supansomboon et al., 2008) and TiN (Reinholdt et al., 2004) also possess properties that can generate a plasmon resonance in the visible, but their relatively large extinction coefficients attenuate the resulting peaks. This leaves Ag and Au as the optimum candidates for application in water or air. Actually, even Ag oxidizes in air, albeit slowly, so care would need to be taken in any applications using this material to protect or passivate the particles.

Results and Discussion

Initial simulations found the frequency of the plasmon resonance to be very sensitive to aspect ratio, as reported for nanorice by Wang *et al*. (Wang et al., 2006). An example for a particle size of L_1 = 40 nm, L_2 = 50nm, L_3 = 32 nm is given in Figure 2(a). As the core size increases (an increase in aspect ratio, *i.e*. the particle becomes more like a shell with an over-all lower volume of metal), the color red-shifts. Jackson and Halas (Jackson and Halas, 2001) reported that the extinction peak shifted to the blue when the shell thickness was increased and the size of the dielectric cores kept constant. In our case, the combination of the shell thickness decreasing and the dielectric core increasing has resulted in a red-shift. The interesting result here is the sudden increase in this red-shift as the aspect ratio changes from 0.5 to 0.7 in both the Ag and Au particles. In the case of the Ag, this shift is associated with a drop in Q_{ext} intensity. In general, the wavelength of the peak extinction of hollow objects exhibits a rapidly increasing sensitivity to aspect ratio as the point of singularity (aspect ratio=1.0) is approached. An example of this is shown in Figure 2(c), for a simple 40 nm outer diameter gold nanoshell, in vacuum. There are, however, practical limits in regard to how thin a shell can be actually synthesized. In addition, significant electron scattering will be experienced for aspect ratio>0.9 anyway, leading to an attenuation of the extinction peaks (Blaber et al., 2009).

Overall, the Ag shell has greater color variability in comparison with the Au particle. The reason for this is that the extinction peaks of the Ag nanoparticles move across the visible, from blue to red end, whereas those of the gold, only start in the mid-visible and move out into the infra red. A comprehensive set of simulations was then undertaken on selected aspect ratios. As the aspect ratio of the shell approaches the extreme (for example, a very thin shell with an aspect ratio of 0.9), it was found that the sensitivity of the color tunability decreased significantly. This is primarily because the main plasmon resonance has been shifted in these instances into the near-infrared and is hence invisible to the eye. However, for an aspect ratio of 0.5, the sensitivity of color to geometry was extensive. Figure 3 shows the resulting color tunability for a particle with variable L_2, constant L_1 (40 nm), L_3 (32

nm) and aspect ratio of 0.5. Figure 4 expands the geometry sensitivity by releasing both L_2 and L_3, while holding L_1 (40 nm) and aspect ratio (0.5) constant for Ag and Au. This can be directly compared with the results in Figures 5 and 6 which were generated for particles with an aspect ratio of 0.3 and 0.7 respectively. For the aspect ratios in the 0.3 to 0.5 range, silver ellipsoids with $L_1 \approx L_2 \approx L_3$, representing a more spherical shape, produce a yellow plasmon resonance directly comparable with the color found associated with Ag nanospheres (Lui and Guyot-Sionnest, 2004). However, as the ellipsoid is elongated, the plasmon resonance red shifts, causing the color transmitted to shift towards blue. It can also be seen that for the thicker shells (*i.e.* approaching a solid nanoparticle), in Figures 4 and 5 the color produced is extremely sensitive to the length parameters. However, as the shell becomes quite thin (Figure 6), the influence of the length parameters is greatly reduced as the plasmon resonance shifts into the near-infrared.

The results are combined in Figure 7, where the shell thickness variation is compared with a variation in L_2 and L_3 (L_1 is fixed at 40 nm), for both Ag and Au. Once again, it can be seen that the Ag shell has far greater color variability in comparison with Au. For an aspect ratio of 0.5, a spherical Ag particle is yellow in color, and it has the singular plasmon resonance of an isolated Ag sphere. Elongating this particle (keeping the volume constant) results in either two or three resonance peaks that are red-shifted in comparison with the plasmon resonance of the spherical particle, and produces a blue color in transmission. As the sphere elongates (for example, L_1= 40 nm, L_2=20 nm, L_3=40 nm) to give a volume decrease, and the resonance peaks blue-shift. If the elongated particle has an increase in the volume (for example, L_1= 40 nm, L_2=60 nm, L_3=40 nm), then the resulting resonance is red-shifted. For the higher aspect ratios of 0.6, 0.7 and 0.8 in Figure 7, L_1 is 40 nm, while L_2 and L_3 are varied in order to produce a particle with constant volume. At an aspect ratio of 0.6, the spherical Ag particle (for example, L_1=L_2=L_3=40 nm) is still yellow in color. However, by 0.7, the particle is becoming more shell-like and the plasmon resonance of the spherical particle is red-shifted. Over-all, as the aspect ratio

increases in the Ag particles, the variability in the color produced by a change in the shape of a particle is significantly diminished.

Finally, we concede that the synthesis of *hollow* particles might be difficult, so it is important to also consider the tunability of core-shell ellipsoids, which are more readily fabricated. The metal shell could be combined with any material, including a second metal, or an entirely difference material, for example, an organic core. In order to simulate this, Ag (with the superior tunability) was chosen as the shell material, and the refractive index of the hypothetical core material was varied (n=1.3, 1.37, 1.40, 1.45 and 1.50) (note: the absorption coefficient, k, has been kept constant at 0 for these calculations). The results are shown in Figure 8. It can be seen that there is minimal change (a slight blue-shift) in the plasmon resonances of the ellipsoid particle, as the refractive index of the core is increased. This suggests that the optical response of the particle in this case is dominated by the metal shell.

Conclusion

Our simulations show that colloidal suspensions of hollow silver scalene nano-ellipsoids with aspect ratios in the 0.3 to 0.5 range will exhibit a very extensive range of color as a function of small changes in length parameters. Furthermore, Ag and Au are the optimum materials from which these colorful nanoparticles might be constructed. The resulting gamut is wide and intense, particularly in the case of the Ag particles. The simulations have confirmed that the aspect ratio is the most influential parameter. The length parameters affect the color produced in shells with aspect ratios in the range of 0.3 to 0.5, but are less critical outside of that range. Hollow scalene ellipsoids have the potential to be the ultimate tunable colloidal particles, with multiple degrees of geometric freedom. However, given the extreme sensitivity that the optical properties of these particles have in relation to their geometry, synthesis of these materials would need to be controlled to a level that is perhaps not yet practical.

References

American Society for Testing and Materials A (2001) E308-01 Standard Practice for Computing the Colors of Objects by using the CIE SystemMaterials.

Blaber MG, Arnold MD, Ford MJ (2009) Search for the iIdeal plasmonic nanoshell: the effects of surface scattering and alternatives to gold and silver J. Phys. Chem. C 113:3041-3045.

Blaber MG, Arnold MD, Harris N, Ford MJ, Cortie MB (2007) Plasmon absorption in nanospheres: a comparison of sodium, potassium, aluminium, silver and gold Phys. B 394:184-187.

Brioude A, Jiang XC, Pileni MP (2005) Optical Properites of gold nanorods:DDA simulations supported by experiments J. Phys. Chem. B 109:13138-13142.

Cortie MB, Xu X, Ford MJ (2006) Effect of composition and packing configuration on the dichroic optical properties of coinage metal nanorods Phys. Chem. Chem. Phys. 8:3520-3527.

Draine BT, Flatau PJ (1994) Discrete-dipole approximation for scattering calculations J. Opt. Soc. Am. A 11:1491-1499.

Draine BT, Flatau PJ (2004) User Guide to the Discrete Dipole Approximation Code DDSCAT 6.1.

Felidj N, Aubard J, Levi G (1999) Discrete dipole approximation for ultraviolet-visible extinction spectra simulation of silver and gold colloids J. Chem. Phys. 111:1195-1208.

He Y, Shi G (2005) Surface plasmon resonances of silver triangle nanoplates: graphic assignments of resonance modes and linear fittings of resonance peaks J Phys. Chem. B 109:17503-17511.

Jackson JB, Halas NJ (2001) Silver nanoshells: variations in morphologies and optical properties J. Phys. Chem. B 105:2743-2746.

Kelly KL, Coronado E, Zhao LL, Schatz GC (2003) The optical properties of metal nanoparticles: the influence of size, shape and dielectric environment J. Phys. Chem. B 107:668-677.

Lui M, Guyot-Sionnest P (2004) Synthesis and optical characterization of Au/Ag core/shell nanorods J. Phys. Chem. B 108:5882-5888.

Oldenburg SJ, Averitt RD, Westcott SL, Halas NJ (1998) Nanoengineering of optical resonances Chem. Phys. Lett. 288:243-247.

Pascale D (2003) A review of RGB color spaces - from xyY to R'G'B'. Montreal, Canada.

Perez-Juste J, Pastoriza-Santos I, Liz-Marzan LM, Mulvaney P (2005) Gold nanorods: synthesis, characterization and applications Coord. Chem. Rev. 249:1870-1901.

Prodan E, Nordlander P (2004) Plasmon hybridization in spherical nanoparticles J. Chem. Phys. 120:5444-5454.

Reinholdt A, Pecenka R, Pinchuk A, Runte S, Stepanov AL, Weirich TE, Kreibig U (2004) Structural, compositional, optical and colorimetric characterization of TiN-nanoparticles Euro. Phys. J. D 31:69-76.

Supansomboon S, Maaroof A, Cortie MB (2008) “Purple glory”: The optical properties and technology of AuAl2 coatings Gold Bull. 41:296-304.

Wang H, Brandl DW, Lel F, Nordlander P, Halas NJ (2006) Nanorice: a hybrid plasmonic nanostructure Nano Lett. 6:827-832.

Weaver JH, Frederikse HPR (2001) IN LIDE, D. R. (Ed.) *CRC Handbook of Chemistry and Physics.* 82 ed. Boca Raton, Florida, CRC Press.

Yu Y-Y, Chang SS, Lee C-L, Chris Wang CR (1997) Gold nanorods: electrochemical synthesis and optical properties J Phys. Chem. B 101:6661-6664.

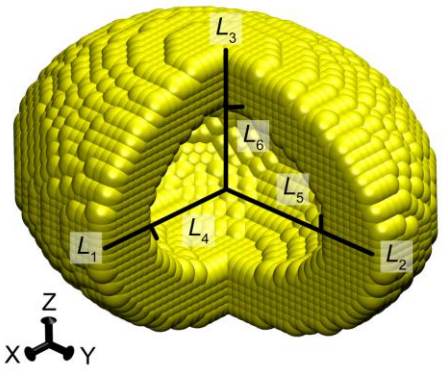

(a)

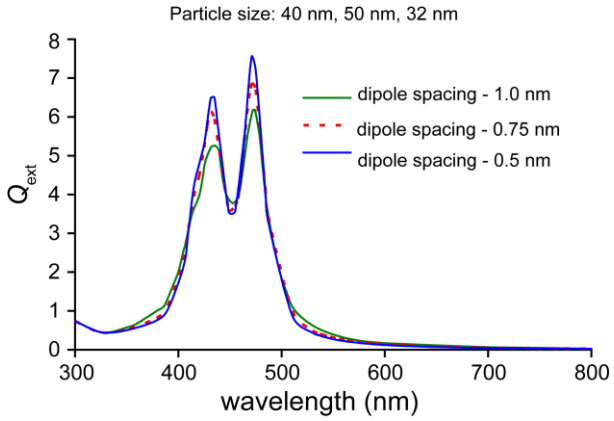

(b)

Figure 1. Typical target and the effect of dipole spacing. (a) Hollowed-out concentric ellipsoidal model used for all calculations. Outer dimensions L_1, L_2 and L_3 are freely variable. Inner shell dimensions L_4, L_5 and L_6 are obtained from the corresponding outer shell dimensions by multiplying with the relevant aspect ratio. Note: L_1 was held constant at 40 nm for this work. The dipoles used to represent the shape in the calculation are shown as little spheres. (b) Effect of dipole spacing on intensity of optical extinction peaks. A particle with size as indicated was considered, and the dipole spacing varied from 1 nm to 0.5 nm. The effect is to slightly attenuate the optical extinction peaks.

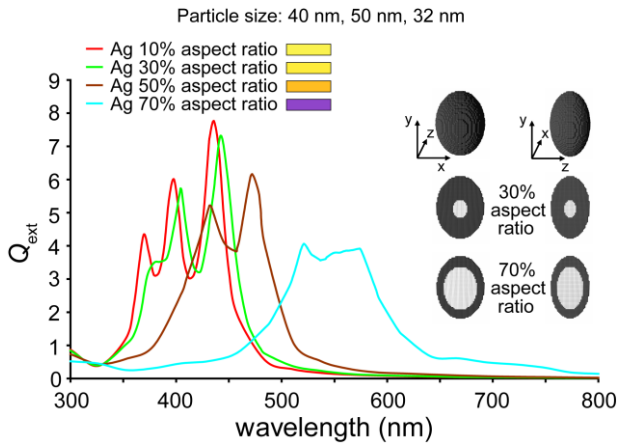

(a)

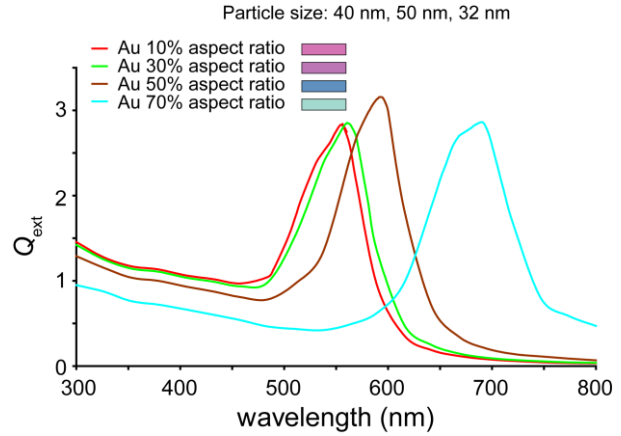

(b)

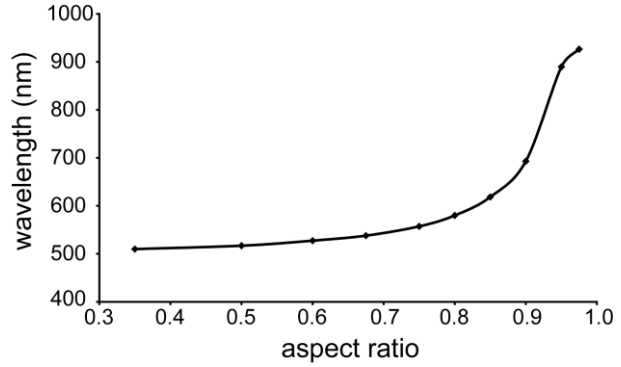

(c)

Figure 2. Extinction efficiencies and resulting colors for particles with outer dimensions of 40 nm, 50 nm and 32 nm, where the aspect ratio has been varied. (a) Ag nanoparticles. (b) Au nanoparticles. (c) Wavelength of the peak extinction of a 40 nm outer diameter gold nanoshell (in vacuum), as a function of increasing aspect ratio.

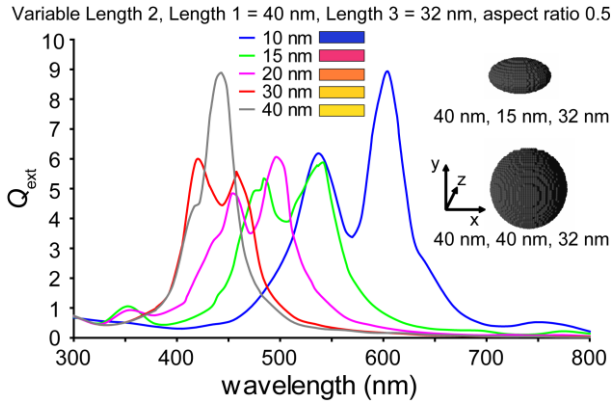

(a)

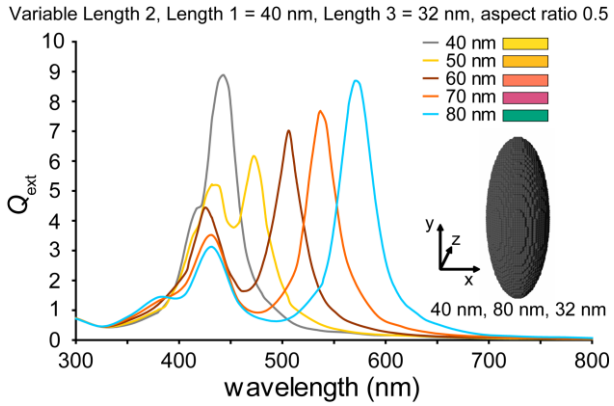

(b)

Figure 3 Extinction efficiencies and resulting colors (small boxes) for a Ag particle with L_2 varied (some examples of the particle shapes are shown) for an aspect ratio of 0.5. (a) particles with $L_2<L_1$, (b) particles with $L_1>L_2$.

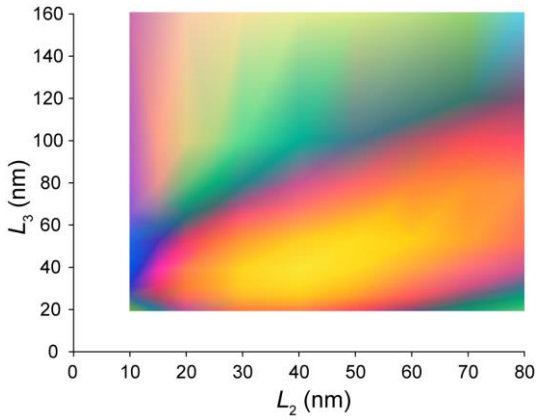

(a)

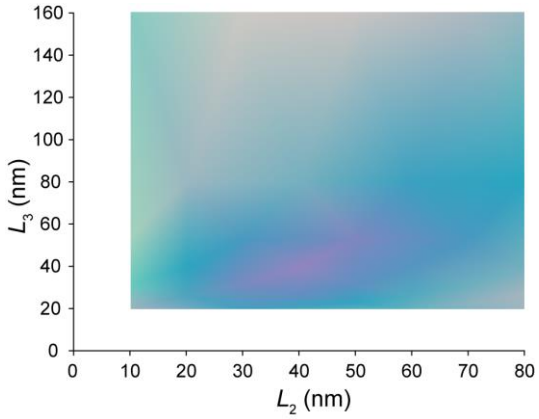

(b)

Figure 4 Color tunability in particles with an aspect ratio of 0.5, with variable L_2 and L_3. (a) Ag nanoparticles. (b) Au nanoparticles.

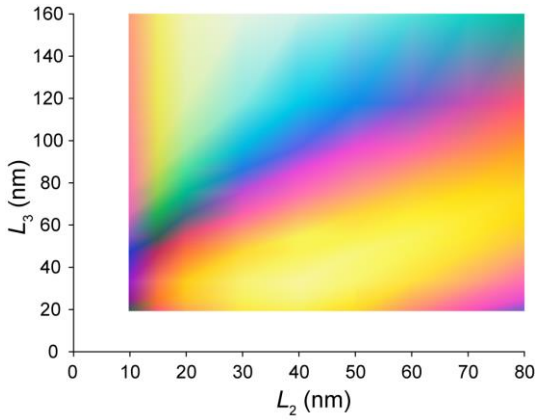

(a)

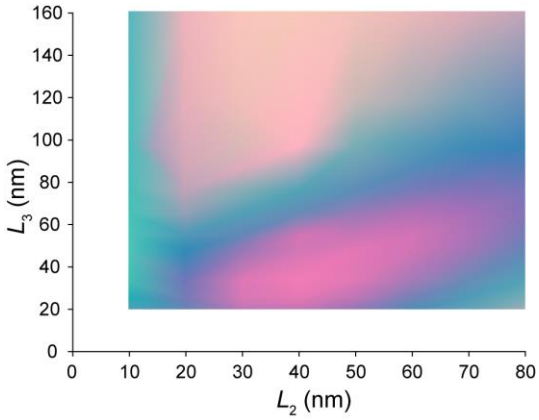

(b)

Figure 5 Color tunability from an aspect ratio of 0.3, with variable L_2 and L_3. (a) Ag nanoparticles. (b) Au nanoparticles.

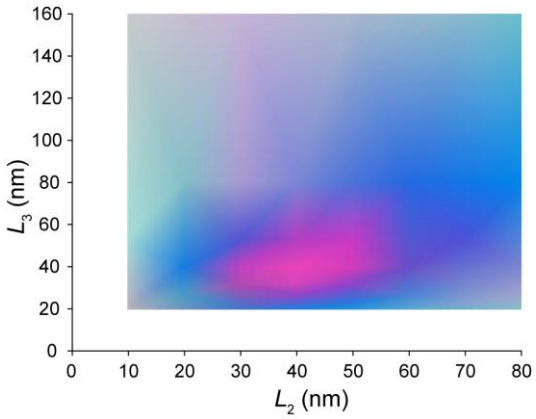

(a)

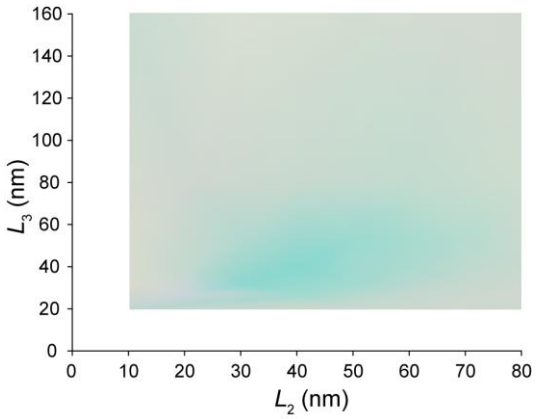

(b)

Figure 6 Color tunability from an aspect ratio of 0.7, with variable L_2 and L_3. (a) Ag nanoparticles. (b) Au nanoparticles.

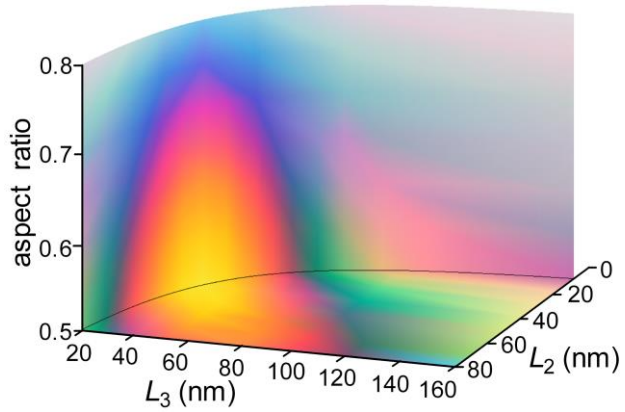

(a)

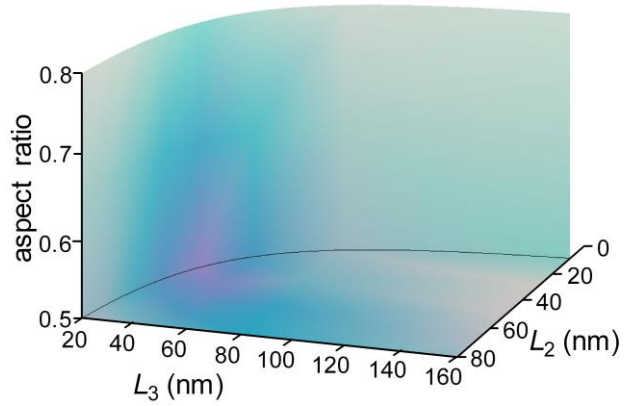

(b)

Figure 7 Gamut of color obtained by variation of L_2 , L_3 and aspect ratio for a) Ag and b) Au. L_1 fixed at 40 nm, L_2 and aspect ratio as shown, and L_3 varied in order to produce a particle with constant volume. Colors have been calculated for 3×10^{16} nanoparticles per m^3.

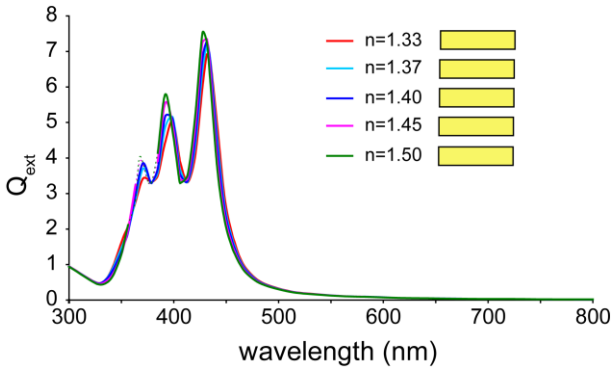

Figure 8 Extinction efficiencies and resulting colors (small boxes) for a particle with outer dimensions of 40 nm, 50 nm and 32 nm, and an aspect ratio 0.5, with variability in the refractive index of the core material. Note: dotted line interpolates a region in which the software used would not converge.